Inter-core Crosstalk Dependence on Design Parameters in Coherent Detection Weakly-Coupled Multicore Fiber Systems

Bruno R. P. Pinheiro[1,2], **João L. Rebola**[1,2], **Adolfo V. T. Cartaxo**[1,2]

[1]*Optical Communications and Photonics Group, Instituto de Telecomunicações, Lisboa, Portugal*

[2] *ISCTE-Instituto Universitário de Lisboa, Lisboa, Portugal*

e-mail: bruno_pinheiro@iscte-iul.pt, joao.rebola@iscte-iul.pt, adolfo.cartaxo@iscte-iul.pt

ABSTRACT

We assess, through numerical simulation, the dependence of the variance of the inter-core crosstalk (ICXT) and the maximum allowable ICXT level on the design parameters of coherent detection MCF systems. The analysed design parameters are the order of the quadrature amplitude modulation (QAM) signals, roll-off factor, time misalignment between the signal in different cores and skew between cores. The results show that, when the roll-off factor is 0, the maximum allowable ICXT level is independent of the skew and decreases for higher QAM orders. For a roll-off factor of 1, the maximum allowable ICXT level depends on the skew and time misalignment of core signals. In this case, the maximum allowable ICXT level increases by 3.6 dB relative to the case of roll-off factor of 0 with null skew, and by 2 dB, when the skew is much higher than the symbol period.

Keywords: coherent detection, inter-core crosstalk, Monte-Carlo simulation, multicore fiber.

1. INTRODUCTION

The multi-core fiber (MCF) has been studied as a transmission media for space division multiplexing in order to overcome the ever-increasing demand for transmission capacity in telecommunication networks [1]. MCF is composed of several spatially separated cores, that can be weakly or strongly coupled [2]. The performance of the optical networks using weakly-coupled MCFs can be highly impaired by inter-core crosstalk (ICXT) [1],[2]. The influence of the ICXT on the performance of MCF systems has been studied in several works [3-4]. In [3] is proposed a theoretical model of the behaviour of ICXT. This model allows to study the influence of ICXT on the performance degradation of MCF systems, and for different modulations formats as those that are typically used in coherent detection, as studied in [3] and [4]. In [5], the ICXT model presented in [3] is improved by considering the dual-polarization ICXT and its dependence on the group velocity dispersion and skew between cores. Despite the influence of the QAM order on the performance of coherent detection MCF system is studied in [4] and [5], the impact on the optical signal-to-noise (OSNR) penalty due to the roll-off factor and the time misalignment between the signals transmitted in the MCF cores is still to be assessed.

In this work, we numerically study through Monte-Carlo (MC) simulation, the variance of the coherently detect ICXT and the influence of ICXT on the OSNR penalty of the coherent detection MCF system, considering different orders of quadrature amplitude modulation (QAM) signals with raised-cosine (RC) pulse shape, roll-off factors, fiber core skews and with time misalignments between the signals transmitted in each MCF core, thereby, extending the results of [4].

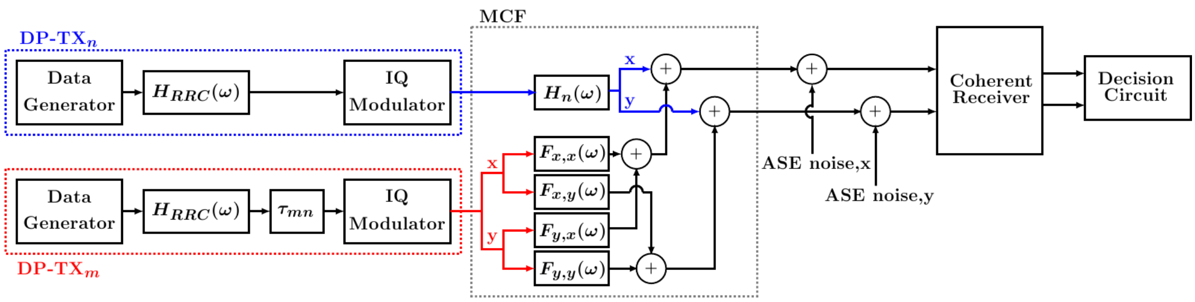

Figure 1. Equivalent simulation model of the MCF system used in this work.

2. SYSTEM SIMULATION MODEL

Figure 1 depicts the simulation model used to assess the dependence of the ICXT on the design parameters of the coherent detection MCF system. The core n is the tested core and the interfering core is core m. Both cores are fed by the corresponding dual polarization-transmitter (DP-TX). Each DP-TX produces, in the data generator, a polarization-division multiplexing (PDM)-M-QAM symbol sequence. Then, each sequence is filtered by a root raised-cosine (RRC) filter, $H_{RRC}(\omega)$, with transfer function $\sqrt{H_{RC}(\omega)}$, where $H_{RC}(\omega)$ denotes the transfer function of the RC filter, presented in [6], and ω is the angular frequency. The in-phase (I) and quadrature (Q) modulator converts the M-QAM electrical signal to the optical domain. These optical signals are transmitted in the corresponding MCF core. To simulate the time difference between the transmission of the optical signals at the MCF input, a τ_{mn} delay is considered in the electrical signal of the DP-TX launched in core m.

The propagation of the signal in core n is modelled by the transfer function $H_n(\omega) = e^{-j\bar{\beta}_n(\omega)L}$, where $\bar{\beta}_n(\omega)$ is the average of the propagation constants of core n and L is the length of the MCF. A Taylor series expansion up to the 2nd order of $\bar{\beta}_n(\omega)$ is considered. In weakly-coupled MCF operating in the phase-matching region, the ICXT signal field in each polarization direction is generated by filtering the signal transmitted in each polarization direction of core m by the transfer function $F_{a,b}(\omega)$ defined as [5]

$$F_{a,b}(\omega) = -j\frac{\bar{K}_{nm}}{\sqrt{2}} e^{-j\bar{\beta}_n(\omega)L} \sum_{k=1}^{N} e^{-j\Delta\bar{\beta}_{mn}(\omega)z_k} e^{-j\phi_{a,b}^{(k)}} \tag{1}$$

where $a,b \in \{\mathbf{x},\mathbf{y}\}$, N is the number of phase-matching points (PMPs), $\bar{K}_{nm}$ is the average of the discrete coupling coefficient over the two polarization directions, and $\Delta\bar{\beta}_{mn}(\omega)$ is the difference between the propagation constant averages of cores m and n given by $\Delta\bar{\beta}_{mn}(\omega) = \Delta\bar{\beta}_{0,mn}+d_{mn}\omega+(\Delta D_{mn}\lambda^2\omega^2)/(4\pi c)$, where $\Delta\bar{\beta}_{0,mn}$ is the difference of propagation constant averages at zero frequency, d_{mn} is the walkoff parameter between cores m and n, ΔD_{mn} is the difference of the dispersion parameters of core m and core n, c is the speed of light in a vacuum, and λ is the wavelength [7]. In this work, $\Delta\bar{\beta}_{0,mn}$ and ΔD_{mn} are 0. The skew, S_{mn}, between the cores m and n is given by $d_{mn}L$. The angle $\phi_{a,b}^{(k)}$ represents the k-th random phase-shift that occurs between two consecutive PMPs, and is a uniformly distributed random variable between 0 and 2π. z_k is the k-th random coordinate that is uniformly distributed between $(k\text{-}1)L/N$ and kL/N. Eq. (1) assumes that the MCF realizations are obtained at time instants, separated by intervals much longer than the correlation time. The transfer functions $F_{\mathbf{x},\mathbf{x}}(\omega)$ and $F_{\mathbf{y},\mathbf{x}}(\omega)$ model the ICXT from polarizations **x** and **y** of core m to the polarization **x** of the interfered core n, respectively, whereas $F_{\mathbf{x},\mathbf{y}}(\omega)$ and $F_{\mathbf{y},\mathbf{y}}(\omega)$ model the ICXT from polarizations **x** and **y** of core m to the polarization **y** of the interfered core n. The amount of ICXT can be quantified by the ICXT level, X_c, which is related to the parameters of Eq. (1) by $X_c=N|\bar{K}_{nm}|^2$.

We assume that the core loss is compensated by optical amplification. Still, the amplification also adds amplified spontaneous emission (ASE) noise to the signal. This noise field is modelled as additive white Gaussian noise for each polarization direction. The coherent receiver detects the PDM-M-QAM signal and ideally compensates the chromatic dispersion. The detected signal is filtered by $H_{RRC}(\omega)$, to produce a RC signal at the decision circuit input. The model of the coherent receiver is the same as the one presented in Fig. 9 of [8].

The system performance is assessed through MC simulation and the bit error rate (BER) is estimated using direct error counting. The MC simulation starts with the random generation of two different M-QAM symbol sequences for the optical signal transmitted in core m, one for each polarization direction. Then, in each realization of ICXT in the MCF, four different functions $F_{a,b}(\omega)$ are used as filters to obtain the ICXT field in each polarization direction, as shown in Fig. 1. The resulted ICXT fields are added to the transmitted signal in the tested core. In addition, an ASE noise sample function is added to the optical signal in each polarization direction. Then, the resulting signal is passed by the coherent receiver and the BER corresponding to the MCF realization is estimated.

3. RESULTS AND DISCUSSION

In this section, the variance of the coherently detected ICXT, for 4, 16 and 64-QAM formats, different roll-off factors, time misalignments between signals and skew between fiber cores is analysed. In order to quantify the impact of the ICXT on the performance, we estimate the BER, the OSNR penalty and the maximum allowable ICXT level, $X_{c,max}$, which is the X_c that leads to a 1 dB OSNR penalty. The OSNR penalty is defined as the ratio between the required OSNR with ICXT and without ICXT, OSNR_R, to achieve a specific target BER [4]. A hard decision FEC with a target BER of 10^{-3} is assumed [4].

Table 1 shows the MC simulation parameters used to assess the performance of MCF system with coherent receiver impaired by ICXT and ASE noise. The OSNR_R, shown in Table 1, agrees with the theoretical OSNR_R [6]. Two roll-off factors (0 and 1) of the RC signals are used in the simulation results.

Table 1. MC simulation parameters.

Parameter	Value		
Bit rate (R_b) [Gbps]	112		
Order of the M-QAM	4	16	64
Symbol rate (R_s)/polarization [Gbaud]	28	14	9.3
Required OSNR for a BER=10^{-3} [dB]	10.3	14.2	18.3
Roll-off factor (β)	0 and 1		
Skew (S_{mn})	Variable		
Normalized time misalignment ($\tau_{mn}\cdot R_s$)	0 and 0.5		
Number of PMPs	500		
Number of generated symbols per realization	2^{12}		

3.1 Detected ICXT Variance

In this subsection, we study the influence of the modulation format, roll-off factor, skew and time misalignment on the variance of the detected ICXT. Fig. 2 depicts the variance of the ICXT normalized to its maximum value as a function of the skew, S_{mn}, for 4, 16 and 64-QAM formats and β of 0 and 1.

Figs. 2(a) and 2(b) correspond to a normalized time misalignment to the symbol period, respectively, of 0 and 0.5. In Fig. 2, it can be observed that, when $\beta = 0$, the variance of the ICXT is practically constant as a function of the skew and is also independent of the QAM order. In Fig. 2(a), for RC signals with $\beta = 1$ and $\tau_{mn} \cdot R_s = 0$, the variance of the ICXT decreases until a minimum for skews of 25, 50 and 75 ps, respectively, for the 4, 16 and 64-QAM signals. These values of skew correspond to $0.7/R_s$. For higher skew values, the variance of the ICXT shows an oscillatory behaviour and tends to 0.75 for higher skews, regardless the QAM order.

In Fig. 2(b), for $\tau_{mn} \cdot R_s = 0.5$ and $\beta = 1$, the minimum variance of ICXT occurs at skews of zero for 4, 16 and 64--QAM. Then, the variance increases until it reaches its maximum value at 25, 50 and 75 ps for 4,16 and 64-QAM, respectively. From Fig. 2, it can be concluded that the time misalignment between the signals in different cores, leads to a substantial variation of the ICXT variance that can reach one half of the maximum value.

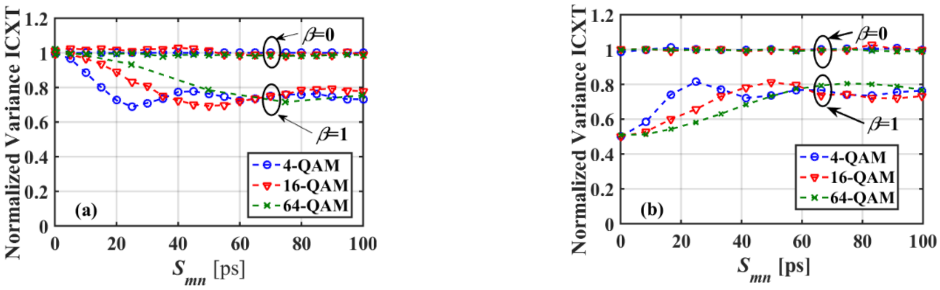

Figure 2. Normalized variance of the ICXT as a function of the skew, roll-off factor of 0 and 1 and (a) $\tau_{mn} \cdot R_s=0$, (b) $\tau_{mn} \cdot R_s=0.5$. 4-QAM (blue), 16-QAM (red) and 64-QAM (green).

3.2 Bit error rate estimation

In this subsection, we estimate the influence of the ICXT generated in each MCF realization on the BER, which we define as BER_r, and obtain the average BER. Fig. 3 depicts the BER_r and the average BER as a function of the number of MCF realizations for different values of skew, time misalignments and roll-off factors, considering the 16-QAM with OSNR of 14.2 dB and an ICXT level of -23 dB. Figs. 3(a)-(c) consider $\tau_{mn} \cdot R_s = 0$, while, in Figs. 3(d)-(f), the $\tau_{mn} \cdot R_s$ is set to 0.5. Figs. 3(a) and (d) consider $\beta = 0$ and $S_{mn} = 0$, Figs. 3(b) and (e) consider $\beta = 0$ and $S_{mn} = 0$ and Figs. 3(c) and (f) consider $\beta = 0$ and $S_{mn} = 160$ ps. The analysis of Fig. 3 shows that the random nature of the ICXT in each MCF realization leads to considerable differences of the BER in each MCF realization. The BER can vary between -1.7 to -3.5. Moreover, as it can be noticed in Fig. 3, the average BER can be considered stable after 200 realizations for all the scenarios of Fig. 3.

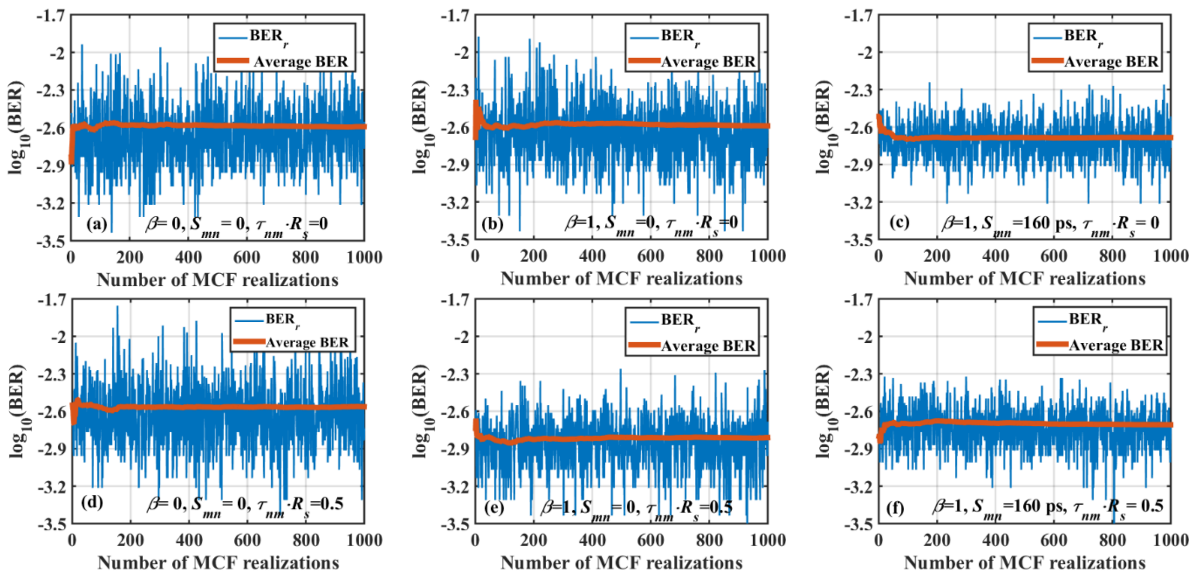

Figure 3: Average BER (red) and BER per MCF realization (blue) as a function of the MCF realization considering 16-QAM with ICXT level =–23 dB and $\tau_{mn} \cdot R_s=0$ (a)-(c) and $\tau_{mn} \cdot R_s=0.5$ (d)-(f).

3.3 Maximum allowable ICXT level

In this subsection, we study the influence of the skew, time misalignment between signals, modulation format orders and signal roll-off factors on the maximum allowable ICXT level in coherent detection MCF systems. Fig. 4 depicts the maximum allowable ICXT level, as a function of the skew for 4, 16 and 64-QAM signals, the roll-off factors of the RC signals and the time misalignment. Fig. 4(a) refers to $\tau_{mn}{\cdot}R_s = 0$, while, in Fig. 4(b), $\tau_{mn}{\cdot}R_s = 0.5$. From Fig. 4, it can be noticed that, when $\beta = 0$ and $\tau_{mn}{\cdot}R_s$ of 0 or 0.5, the maximum allowable ICXT level is practically constant as a function of the skew. The $X_{c,max}$ for RC signals with $\beta = 0$ is –16.7, –23.5 and –30 dB for 4, 16 and 64-QAM, respectively. These results agree with the ones found in [4] and [5]. In Fig. 4(a), it can be observed that, if $\beta = 1$ and skew of 150 ps, the allowable ICXT level improves by 0.7, 1.5 and 2 dB respectively, for 4, 16 and 64-QAM, in comparison to the $X_{c,max}$ values obtained for null skew. In Fig. 3(b), for $\tau_{mn}{\cdot}R_s$=0.5 and $\beta = 1$ shows that with a null skew, the $X_{c,max}$ is 2.4, 3 and 3.6 dB higher than the ones obtained in Fig. 3(a) for the same skew, as the $X_{c,max}$ obtained are –14.3, –20.5 and -26.4 dB for 4, 16, and 64-QAM, correspondingly. For higher skews, it is noticed a $X_{c,max}$ improvement of about 2 dB, regardless the QAM order.

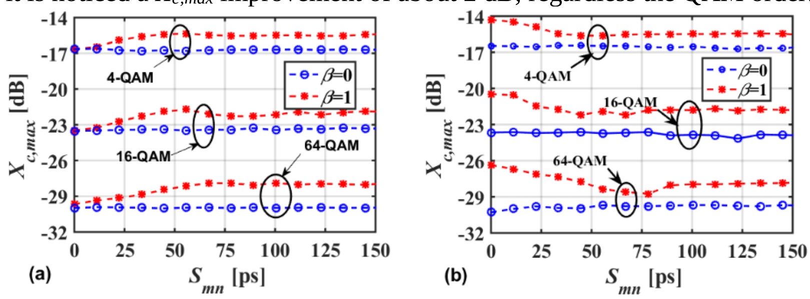

Figure 4: Maximum allowable ICXT level as a function of the skew for 4-QAM, 16-QAM and 64-QAM signals with roll-off factors of $\beta = 0$ and $\beta = 1$ and (a) $\tau_{mn}{\cdot}R_s$=0, (b) $\tau_{mn}{\cdot}R_s$=0.5.

4. CONCLUSIONS

A MC simulator has been developed to estimate the variance of the ICXT and the maximum allowable ICXT level of coherent detection MCF system for 4, 16 and 64-QAM RC signals with different roll-off factors and different time misalignments as a function of the skew. It has been shown that the roll-off factor of 0 leads to a maximum allowable ICXT level independent of the skew and decreases for higher QAM orders. For a roll-off factor of 1, the maximum allowable ICXT level depends on the skew and on the time misalignment of core signals. In this case, the maximum allowable ICXT level increases by 3.6 dB in comparison to the case of roll-off factor of 0 with null skew. When the skew is much higher than the symbol period, the maximum allowable ICXT level increases only by 2 dB. Those results show that, for signals with high roll-off factors, the time misalignment between the transmitted signals maybe used as an ICXT mitigation technique.

ACKNOWLEDGEMENTS

This work was supported in part by Fundação para a Ciência e a Tecnologia (FCT) from Portugal under the project of Instituto de Telecomunicações AMEN-UID/EEA/50008/2013 and the ISCTE-IUL BM-ISCTE-2016.

REFERENCES

[1] W. Klaus *et al.*, “Advanced space division multiplexing technologies for optical networks,” *J. Opt. Commun. Netw.*, vol. 9, no. 4, pp. C1-C11, Apr. 2017.

[2] K. Saitoh, “Multicore fiber technology,” *J. Lightw. Technol.*, vol. 34, no. 1, pp. 55-66, Jan. 1 2016.

[3] T. Hayashi, T. Sasaki, and E. Sasaoka, “Behavior of inter-core crosstalk as a noise and its effect on Q-factor in multi-core fiber,” *IEICE Trans. Commun.*, vol. E97–B, no. 5, pp. 936–944, May 2014.

[4] B. Puttnam *et al.*, “Impact of inter-core crosstalk on the transmission distance of QAM formats in multi-core fibers,” *IEEE Photon. J.*, vol. 8, no. 2, Apr. 2016, Art. no. 0601109.

[5] T. M. F. Alves and A. V. T. Cartaxo, “Intercore crosstalk in homogeneous multicore fibers: theoretical characterization of stochastic time evolution,” *J. Lightw. Technol.*, vol. 35, no. 21, pp. 4613–4623, Nov. 1, 2017.

[6] P. Crilly, and A. B. Carlson, “Communication Systems: An Introduction to Signals and Noise in Electrical Communication,” 4th Ed., McGraw-Hill Education, 2002, ch. 11, sec. 3, p. 463.

[7] A. V. T. Cartaxo *et al.*, “Dispersion impact on the crosstalk amplitude response of homogeneous multi-core fibers,” IEEE Photon. Technol. Lett., vol. 28, no. 17, pp. 1858– 1861, Sep. 2016.

[8] K. Kikuchi, “Fundamentals of coherent optical fiber communications,” *J. Lightw. Technol.*, vol. 34, no. 1, pp. 157–179, Jan. 1 2016.